AMERICAN SCIENTIFIC PUBLISHERS

Science of Advanced Materials
Vol. 12, pp. 853–860, 2020
www.aspbs.com/sam

ARTICLE

Diagnosis of Oral Squamous Cell Carcinoma (OSCC) Using Laser Induced Fluorescence

M. A. N. Razvi[1,*], Ahmed Bakry[1], A. Saeed[1,2], S. M. Afzal[1,5], Y. F. AL-Hadeethi[1], Jaudah AL-Maghrabi[3], and Saad AL-Muhayawi[4]

[1]*Department of Physics, Faculty of Science, King Abdulaziz University, Jeddah 21589, KSA*
[2]*Physics Department, Thamar University, Thamar, 87246, Yemen*
[3]*Department of Pathology, Faculty of Medicine, King Abdulaziz University, Jeddah 21589, KSA*
[4]*Department of Otorhinolaryngology, Faculty of Medicine, King Abdulaziz University, Jeddah 21589, KSA*
[5]*Department of Physics, Aligarh Muslim University, Aligarh 202002, India*

ABSTRACT

Cancer is a dreaded disease; a large number of deaths occur every year due to this disease. Oral squamous cell carcinoma (OSCC) is the most common cancer of the head and neck, which is approximately 16% to 40% of all malignancies. In this study, Laser induced fluorescence (LIF) spectroscopy has been utilized to discriminate OSCC against healthy (normal) tissues and to investigate whether the LIF could provide information from formalin-fixed paraffin-embedded (FFPE) tissue samples similar to that reported using fresh tissues. Samples were prepared after biopsy from ten patients using standard FFPE tissues methods. LIF system consists of a continuous wave (CW) He–Cd laser at 325 nm, a seven-core optical fiber cable coupled to the laser, a spectrometer with cooled charge coupled device (CCD) detector, and a computer for acquisition of the LIF spectra. Spectra were decomposed using second derivative and curve fitting analysis to reveal the changes in molecular composition of the samples. Moreover, samples spectra were discriminated by hierarchical cluster analysis (HCA) and principal components analysis (PCA). Spectral results showed differences in peak areas and positions between normal and OSCC tissues. LIF spectroscopy revealed significant decrease in the peak area of collagen and decrease in peak area of coenzymes of OSCC tissues. In addition, significant shift in the peak position of coenzymes was recorded. HCA and PCA of LIF indicated a very clear discrimination of the normal and FFPE-OSCC tissues. The achieved discrimination between elliptic polygons of normal and OSCC tissues was 96.3% by PCA. This study confirms that the LIF spectroscopy is a good diagnostic tool for OSCC and it could be used with samples that are prepared using FFPE tissues methods.

KEYWORDS: Laser Induced Fluorescence (LIF), Oral Squamous Cell Carcinoma (OSCC), Coenzymes, Collagen, Hierarchical Cluster Analysis (HCA), Principal Components Analysis (PCA).

1. INTRODUCTION

Cancer is a kind of diseases described by uncontrolled production of abnormal cells.[1] It is a dreaded disease and large populations get affected from it, a large number of deaths occur every year due to this disease. According to assessments from the International Agency for Research on Cancer (IARC), around 14.1 million new cancer cases were diagnosed in 2012 worldwide, of which 56.74% were diagnosed in developing countries that contain about 82% of the world's population.[1] These assessments neglected non-melanoma skin cancers that are not tracked in cancer registries.[1] Certain types of cancers have higher incidence in developed world and certain others are more prevalent in the developing nations. In 2012, around 22,000 cancer deaths were recorded per day by cancer worldwide. About 2.9 million were in economically developed countries, whereas 5.3 million were in economically developing countries.[1] The main reason for large number of deaths is the late detection/diagnosis of cancer. Incidence of head and neck cancer is approximately 16% to 40% of all malignancies. Oral squamous cell carcinoma (OSCC) is the most common cancer of the head and neck. In addition, the incidence of OSCC has increased in recent years.[2–5] The OSCC is differentiated only through histologic evaluation. Early diagnosis of cancer is the best way to ensure patient survival and healthy life.[6] If OSCC is detected in the early stages, the disease can be managed better. Hence, there is a need for techniques, which can detect the

*Author to whom correspondence should be addressed.
Email: mrazvi@kau.edu.sa
Received: 14 June 2019
Accepted: 18 September 2019

presence of cancer with high sensitivity, has high discrimination capability and accuracy.

There are many techniques that employ fluorescence spectroscopy measurement such as fluorescence correlation spectroscopy (FCS), photodynamic diagnosis (PDD), photodynamic therapy (PDT), and laser-induced fluorescence (LIF) that are applied to investigate biomedical samples and detect the diseases in biological tissues. The most widespread spectroscopic techniques is LIF, which is mainly used to diagnose the cancer.[7–11] In this technique, laser light is used to illuminate the tissues, and the fluorescence spectrum is collected from the same site.[12–16] There are two ways of collecting the LIF; directly from the naturally occurring tissue endogenous fluorophores (autofluorescence) or by tagging the tissues with a dye-exogenous fluorophore. The second method produces higher fluorescence yield and increases the contrast, however, autofluorescence avoids potential side effects of dyes due to the addition of drugs or dyes. We therefore prefer autofluorescence as our choice. The fluorescence spectra are correlated to the molecular constituents of the tissues. There are subtle differences in the spectra of normal and cancerous regions of the tissues. These occur due to histological changes. The spectra also reflect the metabolic state and concentrations of the constituent fluorescing molecules. One can therefore, discriminate between the tissues through LIF spectroscopy. Hence it is being used as a diagnostic tool that can even be applied *in vivo*; and thus, avoid invasive biopsy.

Recently, LIF has been widely implemented in cancer diagnosis[7, 10, 11, 17] and in particular for *in situ* (*in vivo*) tissue diagnosis. Being a safe technique, it has attracted many physicians to adopt it. Further interesting characteristics are, its a non-invasive approach with excellent sensitivity. The minimal examination period, the minute needed biopsy and *in situ* testing are further distinguished characteristics between premalignant and malignant conditions in certain types of cancers.[8, 16, 18–22]

Using different lasers and wavelengths, LIF spectroscopy studies that were performed to investigate OSCC have been reported in many papers.[16, 23–27] They aimed to discriminate mainly between OSCC and oral normal tissues. Some of the reports that used LIF spectroscopy were carried out *in vivo* tissues; others were carried out using fresh tissues that are kept in saline. Studying *in vivo* is more objective, less time-consuming, and reliable. In addition, there is no need for painful biopsy.[28] In fact, there is a need to test many tissue layers. However, photon excitation that usually operates either UV or visible have a limited penetration depth when applied to biological tissues. Therefore, it is complicated to achieve appropriate either microscopic or spectroscopic analyses at a significant depth into *in vivo* tissues.[29] Of course, keeping fresh tissues in saline is a good method for simulating *in vivo* conditions. However, this often causes major restrictions; as the samples need to be stored at low temperatures else the samples deteriorate rapidly, and there are few other related problems with fresh tissues.[28, 30] On the other hand, there are alternative methods to handle tissues *ex vivo*, such as formalin-fixed paraffin-embedded (FFPE) and formalin-fixing.[30] FFPE tissues methods are the most widely used to store samples in histopathology.[28] Hence, estimation of expediency of fixed samples for LIF spectroscopy has become important. Several studies have investigated the appropriateness of fixation of tissues such as FFPE, formalin fixed in optical histopathology with FTIR, fluorescence, Spectral cytopathology, and Raman technique. These studies were reported in the literatures.[28–34]

In this work, an experimental facility has been setup to implement the LIF diagnosis of OSCC of the tongue tissue samples that are formalin fixed and embedded in paraffin and discriminate them against normal healthy tissues from the same patients. In addition, OSCC tissue was compared to normal tissue with the aim to investigate whether the LIF could provide information from FFPE similar to that were reported from fresh tissue. Details of the setup and the spectral analysis of ten patients are presented in this paper.

2. EXPERIMENTAL DETAILS

2.1. Laser-Induced Fluorescence (LIF) System

A schematic view of the experimental system is shown in Figure 1. The system consists of a continuous wave (CW) helium–cadmium (He–Cd) laser model IK5551 R-F (Kimmon Koha, Japan) working at 325 nm, 60 W. The laser beam is passed through an iris diaphragm to reduce the beam size and a neutral density filter is used to attenuate the power to about few hundred microwatts. The laser beam is coupled to central core of a 7-core optical fiber that irradiates the sample. The fluorescence from the sample is collected by other six cores of the optical fibers are coupled to a spectrometer with cooled charge coupled device (CCD) detector model QEPro (Ocean Optics,

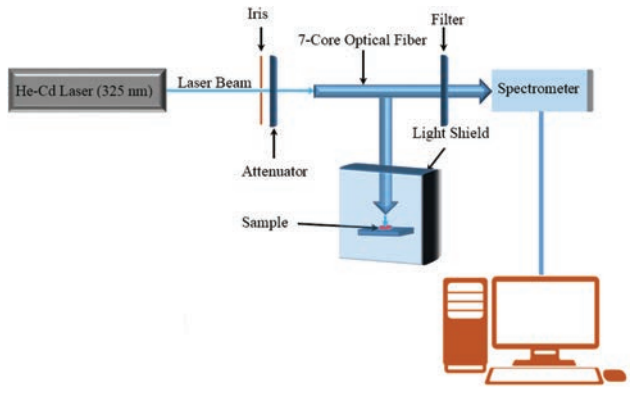

Fig. 1. Schematic of the experimental setup for LIF diagnosis of cancer.

USA). The laser wavelength is filtered out using a Notch filter before it is coupled to the spectrometer.

2.2. Oral Squamous Cell Carcinoma Samples

This is a retrospective study of patients diagnosed with OSCC of the tongue. Cases were retrieved from the archives of the Department of Pathology at King Abdulaziz University, Jeddah, Saudi Arabia. The study was in accordance with the Research Ethic Committee of KAU and according to the ethical guidelines of the 1975 Declaration of Helsinki. All the specimens were fixed in 10% neutral buffered formalin (NBF, approximately 4% formaldehyde). FFPE sections (4 μm) were stained Hematoxylin and eosin. Histopathological diagnosis was reviewed and confirmed by Oncologic Pathologist. Five slides were prepared from OSCC tissues of each patient and five slides for normal tissues of the same patients.

2.3. Recording of Laser-Induced Fluorescence (LIF) Spectra

LIF spectra are recorded from each location and averaged after 500 scans, with 100 ms sampling time and boxcar smoothing of 5 neighbouring points. Hence, total recording takes 50 s to obtain averaged spectrum from each location. Five spectra per slide are recorded at five different positions on the slide. Thus, fifty spectra from every patients (25 OSCC/25 normal) tissues were recorded. Then, every spectrum was processed, where the entire spectrum was baseline corrected in the 350–700 nm regions. Then, the entire spectrum has been min–max normalized by scaling the entire spectrum to the maximum peak. Finally, the average of 25 spectra/patient (five spectra/slide $\times$ five slides/patient) was obtained for both normal and OSCC tissues. Curve fitting and second derivative spectra were used to obtain features of spectral peaks.

2.4. Multivariate Statistical Analysis of the Recorded Spectra

Data from spectral fluorescence of both normal and OSCC tissues were represented as their mean value $\pm$ standard error of the mean (SEM). The differences between them were tested using the t-test for paired measurements. $P < 0.05$ was considered as significant. Multivariate exploratory techniques, specifically, hierarchical cluster analysis (HCA) was used in order to compare the spectral fluorescence of normal and OSCC samples to determine if there were some underlying structural differences. HCA is the simplest and most rapid procedures of cluster analysis that is used to classify data of biological samples. This method is depended on the similarity between two objects.[35,36] Here spectral fluorescence emissions of both normal and OSCC tissues were classified using Wards' method and Euclidean distances. HCA results were presented as dendrograms. Furthermore, Principal components analyses (PCA) were also applied in the spectral fluorescence of both tissues. The PCA is a statistical data diminishing method.[35–39] This method converts the thoroughbred set of variables to a new set of uncorrelated variables. PCA was used to derive a small number of independent linear combinations (principal components). PCA of spectral fluorescence of both normal and OSCC tissues were achieved and graphed based on variance-covariance matrix. HCA and PCA was performed using PAST version 2.17b software.[40] The normalized intensities of fluorescence data from both normal and OSCC tissues of 10 patients extends from 350–700 nm were used for HCA and PCA analyses.

3. RESULTS AND DISCUSSION

3.1. Laser-Induced Fluorescence (LIF) Spectral Analysis

LIF spectra were recorded from each slide at five different locations on the slide. The spectra were baseline corrected and normalized. The average spectra of both normal and OSCC tissues in the range 350–700 nm, of all patients are shown in Figure 2. These average spectra represent baseline corrected, normalized fluorescence spectra that are obtained from 10 patients. In Figure 2, the two spectra of both normal and OSCC tissues are different; there are apparent differences between the normal and cancer tissues spectra in band intensities and a shift is also observed in the band. Two primary fluorescence peaks exist in the spectra. The peak that centers at 387 nm is attributed to fluorescence emission from collagen.[41–45] Collagen fluorescence peak is attributed to cross-links between lysyl pyridinoline and hydroxylysyl pyridoline.[46–48] The broad band that centers around 492 nm, arises mainly from coenzymes: nicotinamide adenine dinucleotide phosphate (NADH), nicotinamide adenine dinucleotide phosphate (NADPH), and flavins[41–45,49–51] that are highly sensitive indicators of metabolic activity. Therefore, they may be specific dynamic markers in tissues and organs.[43,45,52] NADH and NADPH fluorescence results from hydrogen

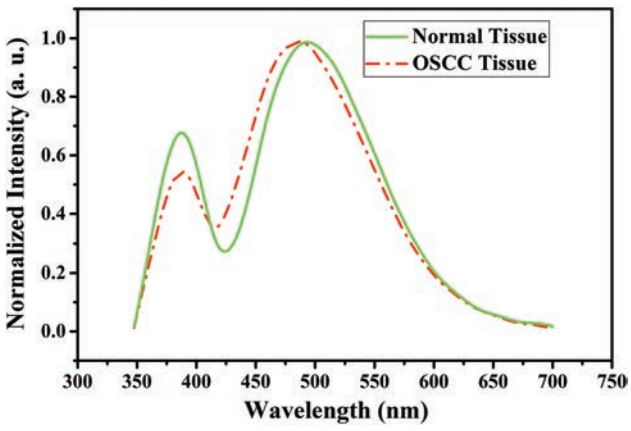

Fig. 2. Average of 250 fluorescence spectra of normal and cancerous tissues of 10 patients.

ARTICLE

Table I. Peak positions and peak areas of fluorescence spectra of normal and cancerous tissues obtained from 10 patients.

	Peak position[a] (nm)		Peak area[a] (a.u.)		Peak FWHM[a] (nm)	
Peak assignment	Normal tissue	OSCC tissue	Normal tissue	OSCC tissue	Normal tissue	OSCC tissue
Collagen	387.65∓0.34	387.73∓0.49	32.40∓2.14	25.25∓1.11[b]	50.22∓0.51	52.14∓0.50[b]
Coenzymes	493.40∓1.49	485.95∓1.65[b]	117.35∓1.76	123.71∓1.98[b]	113.88∓1.35	121.99∓1.77[b]

Notes: [a]Values are expressed as the (mean ± SEM), [b]Significant change in the OSCC tissue compare to normal tissue.

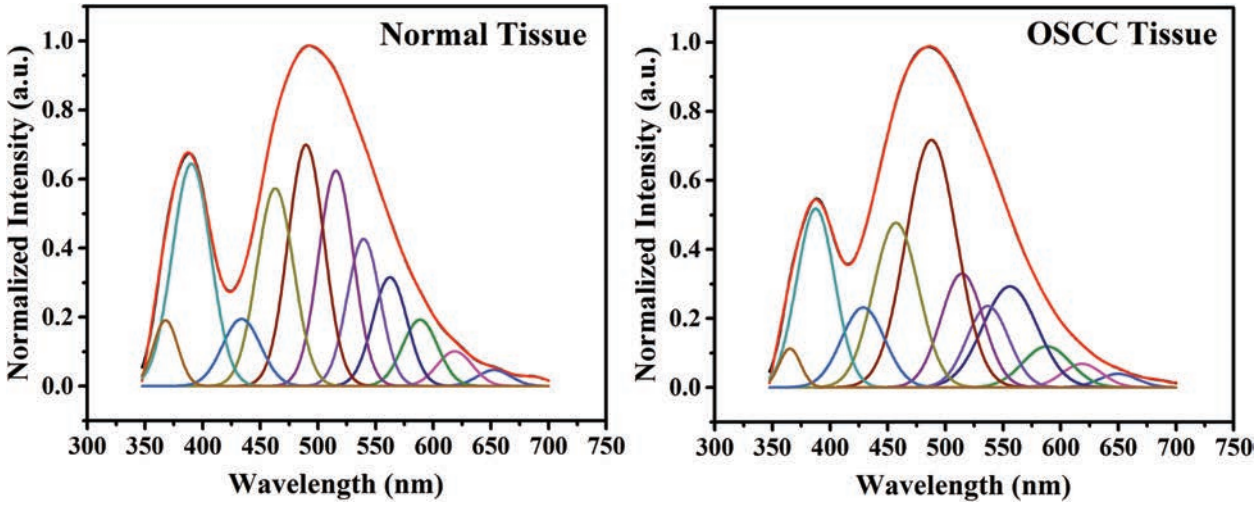

Fig. 3. Curve fitting analysis of fluorescence spectra of average normal and cancerous tissues (10 patients).

uptake at position 4 of its planar pyridine ring[45, 53, 53] However, the fluorescence of flavins can be assigned to energy dispersion by strong interactions of intermolecular contacts[54–56] that are induced by conjugated platforms with polarization of heterocyclic ring system.[54]

From Figure 2, higher intensity of collagen peak can be observed in normal tissues, while it falls and becomes weak in the OSCC tissue. Furthermore, Table I shows the peak center positions, peak areas, and peak full width at half maximum (FWHM) of fluorescence spectra of normal and OSCC tissues. In addition, Table I shows the decrease in collagen of OSCC tissue was significant compared to normal tissue. The significant decrease in collagen suggests that there is probably a decrease in collagen as tissues progress from normal to OSCC state.[40] Table I also shows significant difference between coenzymes peak area of normal and cancerous tissues where there is increase in the coenzymes of OSCC tissue compared to the normal tissue. In addition, Figure 2 and Table I revealed the peak position of fluorescence emission spectra that belongs to coenzymes of OSCC tissue shifted significantly to high frequency (lower wavelength) compared to normal tissues.

Table II. Peak centers of normal and cancerous tissues result from curve fitting.

Peak assignment	Peak centers[a] of normal tissue	Peak centers[a] of OSCC tissue
Collagen	367.61∓0.78	364.50∓1.26[b]
Collagen	389.52∓1.00	388.00∓1.29
Bound NAD(P)H	432.34∓1.16	428.45∓1.27[b]
FeeNAD(P)H	462.71∓0.89	458.70∓0.81[b]
Flavins	490.24∓1.32	487.93∓1.01
Flavins	516.51∓1.92	514.27∓1.76[b]
Flavins	541.08∓2.14	536.37∓3.12
Flavins	559.65∓1.36	556.85∓1.51[b]
Porphyrin	588.10∓1.41	587.89∓1.89
Porphyrin	617.37∓2.10	618.89∓2.69
Porphyrin	652.41∓1.09	649.86∓1.57[b]

[a]Values are expressed as the (mean ± SEM), [b]Significant change in the OSCC tissue compare to normal tissue.

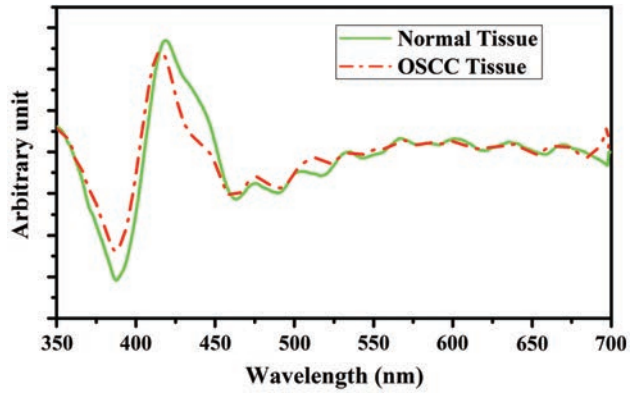

Fig. 4. Second derivative of average fluorescence spectra for both normal and OSCC tissues.

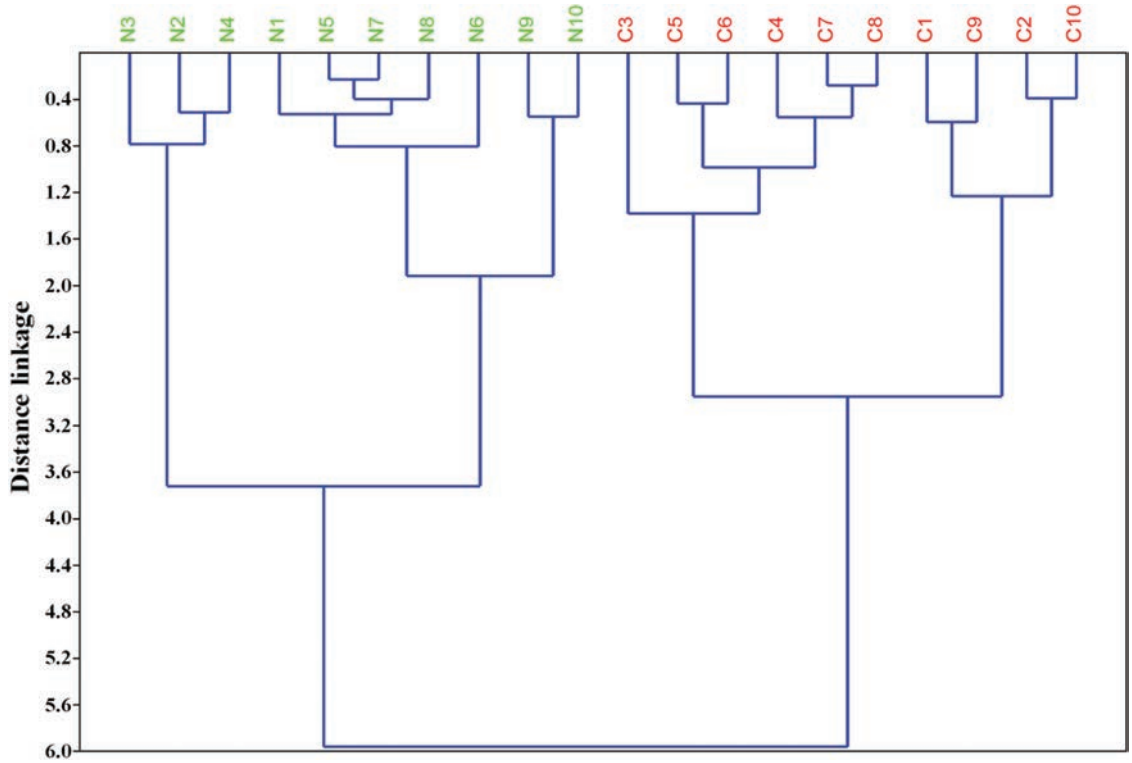

Fig. 5. HCA of fluorescence spectra of normal and OSCC tissues (10 patients).

Table I show that the FWHM of peaks that are attributed to collagen and coenzymes of OSCC tissue increased significantly compared to the normal tissue. Thus, the collagen and coenzymes of OSCC tissue peaks are broader than those peaks belonging to normal tissue. The broadening in collagen and coenzymes of cancerous tissue peaks might result from disordering in the structure of collagen and coenzymes.

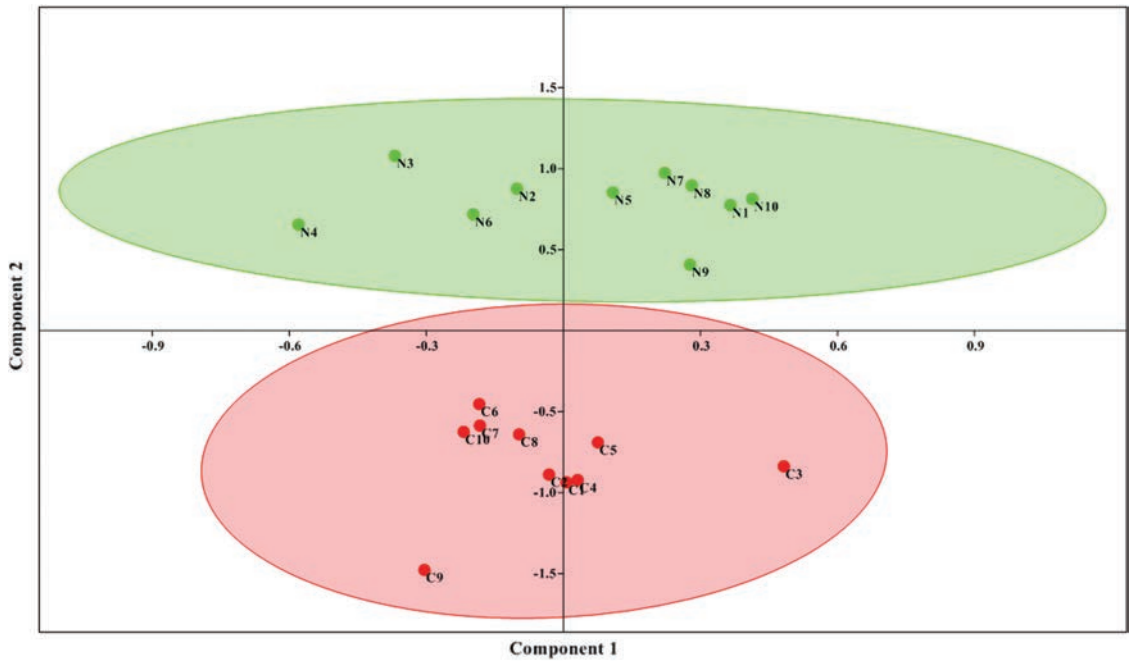

Fig. 6. Scatter plot of the first principal component versus the second principal component after PCA of spectra obtained from normal and OSCC tissues.

ARTICLE

3.2. Curve Fitting and Analysis of Second Derivatives of Spectra

All the fluorescence spectra emissions were subjected to curve fitting to separate overlapping peaks. Curve fitting is a good method for this purpose. Figure 3 shows the typical curve fitting of average fluorescence spectra for both normal and cancerous tissues. From the Figure 3, it is clear that curve fitting revealed many peaks in the spectra. Resultant peaks belong to individual components that make up the spectrum. Curve fitting revealed that there are 11 different peaks in the range 350–700 nm. The peak positions are 366, 388, 430, 460, 489, 515, 538, 558, 587, 618, and 651 nm. The peaks that appeared in the range 350-420 are attributed to collagen[41–43, 56] while the peaks that were observed in the range 430 are attributed to bound NAD(P)H[27, 41, 56] whereas the peaks centered around 460 are attributed to free NAD(P)H.[27, 41–43] The peaks that appeared in the range 480–560 are referred to flavins[41–43, 49, 50] while the peaks that arose in the range 580–650 are imputed to porphyrin.[42, 43, 49, 50, 56]

Table II represents the resultant peaks of curve analysis and shows the significant differences in the cancerous tissue compared to normal tissue. From Table II, it can be seen that there are shift in the resultant peaks of two types of tissues. The peaks of OSCC tissue that have significant differences compared to normal tissue all of them shifted to higher frequency. These are marked with a superscript in the table. Figure 4 shows the second derivative of average fluorescence spectra for both normal and OSCC tissues. It can be seen the different peaks and the shifting that occur in these peaks form the comparison between spectra of normal and OSCC tissues.

3.3. Hierarchical Cluster Analysis (HCA) and Principal Component Analysis (PCA)

The two multivariate statistical analysis techniques used are described in section 2.4 briefly and more details can be found in the references therein. HCA was used to classify fluorescence spectra emission of normal and cancerous tissues from averaged spectra (of 25 normal and 25 cancer tissue spectra) of each individual patient (10 patients). The spectra were in the range (350–700 nm) were analyzed through multivariate exploratory technique to reveal which spectra are most similar to each other. HCA that was done using Ward's algorithm Euclidean distance linkage tree is illustrated in the dendrograms at Figure 5. The dendrograms created two initial clusters represented by two branches, which were further subdivided into smaller clusters. The smaller the distance is required to connect two clusters, the greater the similarity between them. It is apparent from Figure 5, Wards method Euclidean distances dendrogram, linkage tree, succeeded to differentiate between the normal and OSCC tissues. Therefore, the spectra of cancerous tissue can be distinguished from normal tissue very clearly.

In addition, we also used another statistical analytical technique PCA. Principle components are calculated for 10 patients. The scatter plot projection was graphed as in Figure 6. Those scatter plots of the first principal component versus second principal component are found to be separated into two groups. The groups were distinguished as illustrated in the elliptic polygon. This means the normal and OSCC tissues are clearly discriminated in the plots. The achieved discrimination between elliptic polygons of normal and cancerous tissues was 96.3%. PCA has demonstrated a very high discrimination capability for distinguishing between the normal and OSCC tissues.

4. CONCLUSIONS

The experimental facility based on the LIF spectroscopy has been successfully setup and tested. Formalin fixed samples from 10 patients were analyzed by recording large number of spectra from the normal and OSCC tissues of same patients. The spectral analysis showed that there are very clear differences in the intensity and shape of the spectra between the two types of samples. The present study using LIF spectroscopy data was able to discriminate between normal and OSCC tissues. LIF spectroscopy revealed significant decrease in the peak area of OSCC collagen compared to normal tissue. However, significant increase in the peak area of OSCC coenzymes was recorded. These were further analyzed using statistical techniques of HCA and PCA. The two analyses provided a clear discrimination between normal and cancerous oral tissues. This study concluded that the LIF spectroscopy is a good diagnostic tool for OSCC tissues. Moreover, LIF spectroscopy could be used with samples that are prepared using FFPE tissues method.

Acknowledgment: This project was funded by the National Plan for Science, Technology and Innovation (MAARIFAH)—King Abdulaziz City for Science and Technology—the Kingdom of Saudi Arabia—award number 11-BIO1985-03. The authors also, acknowledge with thanks Science and Technology Unit, King Abdulaziz University for technical support.

References and Notes

1. American Cancer Society, Global Cancer Facts and Figures, American Cancer Society, 3rd edn., Atlanta **(2015)**.
2. H. Yang, W. Q. Jiang, Y. Cao, Y. A. Sun, J. Wei, X. An, Y. C. Zhang, M. Song, S. S. Wang, Z. Y. Yuan, R. J. Peng, T. H. Chen, L. R. Li, and Y. X. Shi, Elevated ZNF703 protein expression is an independent unfavorable prognostic factor for survival of the patients with head and neck squamous cell carcinoma. *Dis Markers* 2015, 640263 **(2015)**.
3. J. V. Bagan and C. Scully, Recent advances in oral Oncology 2007: Epidemiology, aetiopathogenesis, diagnosis and prognostication. *Oral Oncology* 44, 103 **(2008)**.
4. B. Wang, S. Zhang, K. Yue, and X.-D. Wang, The recurrence and survival of oral squamous cell carcinoma: A report of 275 cases. *Chin. J. Cancer* 32, 614 **(2013)**.

5. M. A. Ermer, K. Kirsch, G. Bittermann, T. Fretwurst, K. Vach, and M. C. Metzger, Recurrence rate and shift in histopathological differentiation of oral squamous cell carcinoma-–A long-term retrospective study over a period of 13.5 years. *Journal of Cranio-Maxillofacial Surgery* 43, 1309 **(2015)**.
6. J. Karbach, B. Al-Nawas, M. Moergel, and M. Daubländer, Oral health-related quality of life of patients with oral lichen planus, oral leukoplakia, or oral squamous cell carcinoma. *Journal of Oral and Maxillofacial Surgery* 72, 1517 **(2014)**.
7. L. Silveira, J. Â. B. Filho, F. L. Silveira, R. A. Zângaro, and M. T. T. Pacheco, Laser-induced fluorescence at 488 nm excitation for detecting benign and malignant lesions in stomach mucosa. *Journal of Fluorescence* 18, 35 **(2008)**.
8. W. Liu, X. Zhang, K. Liu, S. Zhang, and Y. Duan, Laser-induced fluorescence: Progress and prospective for in vivo cancer diagnosis. *Chin. Sci. Bull.* 58, 2003 **(2013)**.
9. M. Al-Salhi, V. Masilamani, T. Vijmasi, H. Al-Nachawati, and A. P. VijayaRaghavan, Lung cancer detection by native fluorescence spectra of body fluids—A preliminary study. *Journal of Fluorescence* 21, 637 **(2011)**.
10. B. Benmansour, L. Stephan, J.-Y. Cabon, L. Deschamps, and P. Giamarchi, Spectroscopic properties and laser induced fluorescence determination of some endocrine disrupting compounds. *Journal of Fluorescence* 21, 843 **(2011)**.
11. X. Zhang, A. Fales, and T. Vo-Dinh, Time-resolved synchronous fluorescence for biomedical diagnosis. *Sensors (Basel)* 15, 21746 **(2015)**.
12. I. Georgakoudi and M. S. Feld, The combined use of fluorescence, reflectance, and light-scattering spectroscopy for evaluating dysplasia in Barrett's esophagus. *Gastrointestinal Endoscopy Clinics of North America* 14, 519 **(2004)**.
13. D. M. Harris and J. Werkhaven, Endogenous porphyrin fluorescence in tumors. *Lasers in Surgery and Medicine* 7, 467 **(1987)**.
14. N. Ramanujam, Fluorescence spectroscopy of neoplastic and non-neoplastic tissues. *Neoplasia* 2, 89 **(2000)**.
15. T. Vo-Dinh, M. Panjehpour, B. F. Overholt, C. Farris, F. P. B. Iii, and R. Sneed, In vivo cancer diagnosis of the esophagus using differential normalized fluorescence (DNF) indices. *Lasers in Surgery and Medicine* 16, 41 **(1995)**.
16. R. Richards-Kortum, M. F. Mitchell, N. Ramanujam, A. Mahadevan, and S. Thomsen, In vivo fluorescence spectroscopy: Potential for non-invasive, automated diagnosis of cervical intraepithelial neoplasia and use as a surrogate endpoint biomarker. *J. Cell. Biochem.* 56(Suppl. 19), 111 **(1994)**.
17. V. Ducháč, J. Zavadil, J. Vránová, T. Jirásek, J. Štukavec, and L. Horák, Peroperative optical autofluorescence biopsy-verification of its diagnostic potential. *Lasers in Medical Science* 26, 325 **(2011)**.
18. F. Robert, L. Bert, L. Denoroy, and B. Renaud, Capillary zone electrophoresis with laser-induced fluorescence detection for the determination of nanomolar concentrations of noradrenaline and dopamine: Application to brain microdialyzate analysis. *Anal. Chem.* 67, 1838 **(1995)**.
19. F. F. D. C. Marques, A. L. M. C. da Cunha, and R. Q. Aucélio, Laser induced fluorescence and photochemical derivatization for trace determination of camptothecin. *Talanta* 83, 256 **(2010)**.
20. D. Anglos, M. Solomidou, I. Zergioti, V. Zafiropulos, T. G. Papazoglou, and C. Fotakis, Laser-induced fluorescence in artwork diagnostics: An application in pigment analysis. *Appl. Spectrosc.* 50, 1331 **(1996)**.
21. H.-H. Yeh, Y.-H. Yang, and S.-H. Chen, Simultaneous determination of memantine and amantadine in human plasma as fluorescein derivatives by micellar electrokinetic chromatography with laser-induced fluorescence detection and its clinical application. *Electrophoresis* 31, 1903 **(2010)**.
22. A. L. N. Francisco, W. R. Correr, C. A. L. Pinto, J. G. Filho, T. C. Chulam, C. Kurachi, and L. P. Kowalski, Analysis of surgical margins in oral cancer using in situ fluorescence spectroscopy. *Oral Oncology* 50, 593 **(2014)**.
23. B. K. Manjunath, J. Kurein, L. Rao, C. Murali Krishna, M. S. Chidananda, K. Venkatakrishna, and V. B. Kartha, Autofluorescence of oral tissue for optical pathology in oral malignancy. *Journal of Photochemistry and Photobiology B: Biology* 73, 49 **(2004)**.
24. J. L. Jayanthi, R. J. Mallia, S. T. Shiny, K. V. Baiju, A. Mathews, R. Kumar, P. Sebastian, J. Madhavan, G. N. Aparna, and N. Subhash, Discriminant analysis of autofluorescence spectra for classification of oral lesions in vivo. *Lasers in Surgery and Medicine* 41, 345 **(2009)**.
25. A. L. N. Francisco, W. R. Correr, L. H. Azevedo, V. G. Kern, C. A. L. Pinto, L. P. Kowalski, and C. Kurachi, Fluorescence spectroscopy for the detection of potentially malignant disorders and squamous cell carcinoma of the oral cavity. *Photodiagnosis and Photodynamic Therapy* 11, 82 **(2014)**.
26. A. Patil, V. K. Unnikrishnan, R. Bernard, K. M. Pai, R. Ongole, V. B. Kartha, and S. Chidangil, Laser induced fluorescence spectroscopy of soft tissues of the oral cavity. *AIP Conference Proceedings* 1349, 224 **(2011)**.
27. C. M. Krishna, G. D. Sockalingum, L. Venteo, R. A. Bhat, P. Kushtagi, M. Pluot, and M. Manfait, Evaluation of the suitability of ex vivo handled ovarian tissues for optical diagnosis by Raman microspectroscopy. *Biopolymers* 79, 269 **(2005)**.
28. M. G. Xu, E. D. Williams, E. W. Thompson, and M. Gu, Effect of handling and fixation processes on fluorescence spectroscopy of mouse skeletal muscles under two-photon excitation. *Appl. Opt.* 39, 6312 **(2000)**.
29. C. M. Krishna, G. D. Sockalingum, B. M. Vadhiraja, K. Maheedhar, A. C. K. Rao, L. Rao, L. Venteo, M. Pluot, D. J. Fernandes, M. S. Vidyasagar, V. B. Kartha, and M. Manfait, Vibrational spectroscopy studies of formalin-fixed cervix tissues. *Biopolymers* 85, 214 **(2007)**.
30. S. Anand, R. Cicchi, F. Giordano, A. M. Buccoliero, R. Guerrini, and F. S. Pavone, Bimodal spectroscopy of formalin fixed samples to discriminate dysplastic and tumor brain tissues. *Latvian Journal of Physics and Technical Sciences* 51, 14 **(2014)**.
31. A. I. Mazur, E. J. Marcsisin, B. Bird, M. Miljković, and M. Diem, Evaluating different fixation protocols for spectral cytopathology, part 1. *Anal. Chem.* 84, 1259 **(2012)**.
32. C. M. Krishna, G. D. Sockalingum, R. A. Bhat, L. Venteo, P. Kushtagi, M. Pluot, and M. Manfait, FTIR and Raman microspectroscopy of normal, benign, and malignant formalin-fixed ovarian tissues. *Analytical and Bioanalytical Chemistry* 387, 1649 **(2007)**.
33. E. Ó. Faoláin, M. B. Hunter, J. M. Byrne, P. Kelehan, M. McNamara, H. J. Byrne, and F. M. Lyng, A study examining the effects of tissue processing on human tissue sections using vibrational spectroscopy. *Vib. Spectrosc.* 38, 121 **(2005)**.
34. S. S. Nafee, A. Saeed, S. A. Shaheen, S. M. El Assouli, M. Z. E. Assouli, and G. A. Raouf, Effect of very low dose fast neutrons on the DNA of rats' peripheral blood mononuclear cells and leukocytes. *Health Phys.* 110, 50 **(2016)**.
35. A. Saeed, G. A. Raouf, S. S. Nafee, S. A. Shaheen, and Y. Al-Hadeethi, Effects of very low dose fast neutrons on cell membrane and secondary protein structure in rat erythrocytes. *PLoS ONE* 10 **(2015)**.
36. P. Yu, Applications of hierarchical cluster analysis (CLA) and principal component analysis (PCA) in feed structure and feed molecular chemistry research, using synchrotron-based fourier transform infrared (FTIR) microspectroscopy. *J. Agric. Food. Chem.* 53, 7115 **(2005)**.
37. P. Yu, Prediction of protein supply to ruminants from concentrates: Comparison of the NRC-2001 model with the DVE/OEB system. *J. Sci. Food Agric.* 85, 527 **(2005)**.
38. P. Yu, Synchrotron-based microspectroscopic analysis of molecular and biopolymer structures using multivariate techniques and

ARTICLE

advanced multi-components modeling. *Can. J. Anal. Sci. Spectros.* 220 **(2008)**.

39. Ø. Hammer, D. A. T. Harper, and P. D. Ryan, Past: Paleontological statistics software package for education and data analysis. *Palaeontologia Electronica* 4, XIX **(2001)**.

40. C. Pöhlker, J. A. Huffman, and U. Pöschl, Autofluorescence of atmospheric bioaerosols-fluorescent biomolecules and potential interferences. *Atmos. Meas. Tech.* 5, 37 **(2012)**.

41. L. S. Lin, F. W. Yang, and S. S. Xie, Extracting autofluorescence spectral features for diagnosis of nasopharyngeal carcinoma. *Laser Physics* 22, 1431 **(2012)**.

42. M. Viegas, T. C. Martins, F. Seco, and A. Do Carmo, An improved and cost-effective methodology for the reduction of autofluorescence in direct immunofluorescence studies on formalin-fixed paraffin-embedded tissues. *European Journal of Histochemistry* 51, 59 **(2007)**.

43. D. G. Farwell, J. D. Meier, J. Park, Y. Sun, H. Coffman, B. Poirier, J. Phipps, S. Tinling, D. J. Enepekides, and L. Marcu, Time-resolved fluorescence spectroscopy as a diagnostic technique of oral carcinoma: Validation in the hamster buccal pouch model. *Arch. Otolaryngol. Head Neck. Surg.* 136, 126 **(2010)**.

44. J. D. Meier, H. Xie, Y. Sun, Y. Sun, N. Hatami, B. Poirier, L. Marcu, and D. G. Farwell, Time-resolved laser-induced fluorescence spectroscopy as a diagnostic instrument in head and neck carcinoma. *Otolaryngol. Head Neck. Surg.* 142, 838 **(2010)**.

45. D. R. Eyre, M. A. Weis, and J.-J. Wu, Advances in collagen cross-link analysis. *Methods* 45, 65 **(2008)**.

46. D. R. Eyre, M. A. Paz, and P. M. Gallop, Cross-linking in collagen and elastin. *Annu. Rev. Biochem.* 53, 717 **(1984)**.

47. V. V. Roshchina, Autofluorescence of plant secreting cells as a biosensor and bioindicator reaction. *Journal of Fluorescence* 13, 403 **(2003)**.

48. G. Bottiroli and A. C. Croce, Autofluorescence spectroscopy of cells and tissue as a tool for biomedical diagnosis. Lasers and Current Optical Techniques in Biology: The Royal Society of Chemistry, edited by G. Palumbo, R. Pratesi, D.-P. Häder, and G. Jori **(2004)**, pp. 189–210.

49. M. Yoshimura, J. Sugiyama, M. Tsuta, K. Fujita, M. Shibata, M. Kokawa, S. Oshita, and N. Oto, Prediction of aerobic plate count on beef surface using fluorescence fingerprint. *Food and Bioprocess Technology* 7, 1496 **(2014)**.

50. K. Koenig and H. Schneckenburger, Laser-induced autofluorescence for medical diagnosis. *Journal of Fluorescence* 4, 17 **(1994)**.

51. K. König, M. W. Berns, and B. J. Tromberg, Time-resolved and steady-state fluorescence measurements of β-nicotinamide adenine dinucleotide-alcohol dehydrogenase complex during UVA exposure. *Journal of Photochemistry and Photobiology B: Biology* 37, 91 **(1997)**.

52. H. Suzuki, R. Inoue, S. Kawamorita, N. Komiya, Y. Imada, and T. Naota, Highly fluorescent flavins: Rational molecular design for quenching protection based on repulsive and attractive control of molecular alignment. *Chem. Eur. J.* 21, 9171 **(2015)**.

53. S. T. Caldwell, G. Cooke, S. G. Hewage, S. Mabruk, G. Rabani, V. Rotello, B. O. Smith, C. Subramani, and P. Woisel, Model systems for flavoenzyme activity: Intramolecular self-assembly of a flavin derivative via hydrogen bonding and aromatic interactions. *Chem. Commun.* 35, 4126 **(2008)**.

54. M. Gray, A. J. Goodman, J. B. Carroll, K. Bardon, M. Markey, G. Cooke, and V. M. Rotello, Model systems for flavoenzyme activity: Interplay of hydrogen bonding and aromatic stacking in cofactor redox modulation. *Org. Lett.* 6, 385 **(2004)**.

55. S.-Y. Ju and F. Papadimitrakopoulos, Synthesis and redox behavior of flavin mononucleotide-functionalized single-walled carbon nanotubes. *J. Am. Chem. Soc.* 130, 655 **(2008)**.

56. A. C. Croce and G. Bottiroli, Autofluorescence spectroscopy and imaging: A tool for biomedical research and diagnosis. *Eur. J. Histochem.* 58, 2461 **(2014)**.